Charge Asymmetry of Weak Boson Production at the LHC and the Charm Content of the Proton

Francis Halzen

Wisconsin IceCube Particle Astrophysics Center and Department of Physics, University of Wisconsin, Madison, WI, 53706

Yu Seon Jeong and C. S. Kim*

Department of Physics and IPAP, Yonsei University, Seoul 120-749, Korea

Abstract

We investigate the production of the weak bosons W^+, W^- and Z at the LHC as a function of their rapidity, reconstructed *experimentally* from their leptonic decay. We show that the measurements provide a powerful tool for constraining the parton distribution functions, as was already the case for the lower energy $p\bar{p}$ collider data. We study the charge asymmetry determining the u and d distribution functions using the reconstructed W^+, W^- rapidities. We also show how the ratio of the W and Z boson rapidity distributions directly probes the charm quark distribution function of the proton.

PACS numbers:

* cskim@yonsei.ac.kr

I. INTRODUCTION

The weak bosons W^+, W^- and Z are produced in a hadron collider predominantly through the interaction of a quark and antiquark from each hadron, the so-called Drell-Yan mechanism [1]. This process has been studied extensively as a test the Standard Model (SM) [2–17].

The cross sections for $W^{\pm}$, Z production have been computed in quantum chromodynamics (QCD) up to the next-to-next-to leading order (NNLO) [18, 19] and provide a test of higher order QCD corrections. The measured cross sections are related to the partonic QCD cross sections by the parton distribution functions (PDFs). The partonic cross sections and the PDFs factorize making a direct study of the PDFs possible.

Particularly, the PDFs can be examined using the rapidity dependence of the W and Z production cross sections. The method is familiar from the analysis of lower energy $p\bar{p}$ collider data [20] where it has been extensively used to investigate the $u(x)$ and $d(x)$ distributions using the ratio of the W^+ and W^- rapidity distributions, referred to as the charge asymmetry [20–25]. Additionally a prescription was proposed to determine the charm quark structure function from both W and Z rapidity distributions measured at the Tevatron [26], where the charm quark contribution to W, Z production is small. Using a similar method, the strange quark distribution has been studied at the LHC [27, 28].

In this paper, we investigate the PDFs by applying the same methods [20, 26] to W and Z rapidity distributions at the LHC center of mass energy $\sqrt{s} = 7$ TeV, to be increased to 14 TeV in the future. These are significantly higher energies than the Tevatron energy of $\sqrt{s} = 1.8$ TeV for Run I and 1.96 for Run II. The higher energy not only leads to increased production rates, it provides access to the lower fractional momenta of the partons where sea quark interactions dominate; these were difficult to probe at Tevatron energies. We will return to this later on. In addition to the increased energy, the LHC collides protons, a symmetric process, resulting in a different pattern of rapidity distributions and charge asymmetry compared to $p\bar{p}$ collisions. Specifically, using the charge asymmetry and the ratio of the W and Z boson rapidity distributions, we will show how the LHC data, unlike the lower energy Tevatron data, directly probe $u(x)/d(x)$ and the charm quark distribution function, respectively.

This paper is organized as follows. In the following section, we introduce the formalism.

In Section III, we investigate the $u(x)$, $d(x)$ PDFs using the charge asymmetry of the experimentally reconstructed W^+ and W^- rapidity distributions. In Section IV, we demonstrate the sensitivity of the charm quark PDF to the ratio of the rapidity dependence of the W and Z cross section. Finally, in Section V, we summarize our results.

II. RAPIDITY DISTRIBUTIONS OF THE DIFFERENTIAL CROSS SECTIONS

The general expression for the cross sections for W, Z production is given by

$$\sigma_{AB\to W/Z} = \sum_{a,b} \int dx_a \int dx_b f_{a/A}(x_a, Q^2) f_{b/B}(x_b, Q^2) \hat{\sigma}_{ab\to W/Z} \ , \tag{1}$$

where the partonic scattering cross section is $\hat{\sigma}_{ab\to W/Z}$. In Eq. 1, $x_{a(b)}$ are the momentum fractions carried by the partons $a(b)$ in the colliding hadrons $A(B)$, and $f_{a/A}(x_a, Q^2)$ and $f_{b/B}(x_b, Q^2)$ are the PDFs of a and b, respectively. The scale Q^2 is set to be the mass squared of the produced boson, $Q^2 = M^2_{W/Z}$.

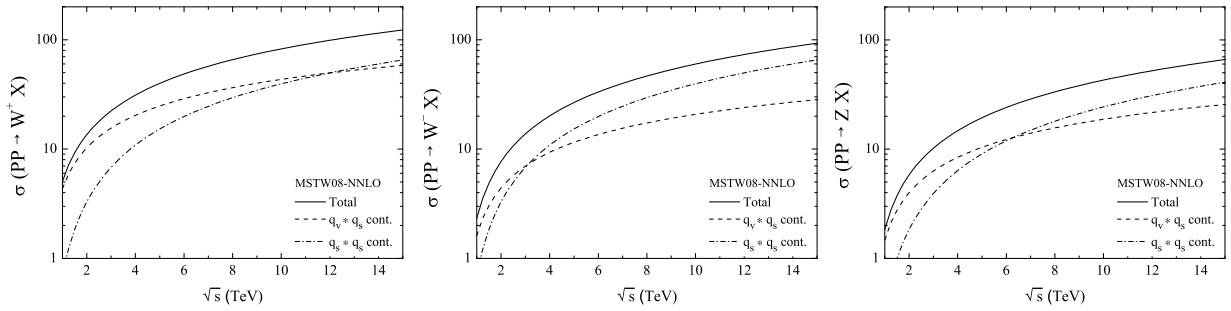

FIG. 1: The total cross sections for the production of weak bosons, $W^{+(-)}$ and Z in proton-proton collision. The separate contributions from the valence-sea (dashed) and the sea-sea (dot-dashed) interactions are also shown as function of energy.

In Fig. 1, we have calculated the cross sections for inclusive W, Z production using the VRAP [19] program. The cross sections are evaluated to NNLO using the MSTW2008-NNLO set of PDFs [29]. The total cross section for W^+ production is different from that for W^- production while they are identical in $p\bar{p}$ collision. The separate contributions from the valence-sea and sea-sea quark interactions are also included. Since there is no contribution from valence-valence quark interactions for pp collisions, the role of the sea quarks is enhanced and, as energy increases, the sea quark contributions become increasingly important. They are responsible for the increased production of W^- and Z relative to W^+.

In addition to the total cross section, we are here particularly interested in the differential cross sections as a function of rapidity that sample the momentum fractions of the partons and are therefore optimal for constraining the PDFs. Including the heavy quark flavors, the differential cross section for W and Z boson production in pp collisions are given by

$$\begin{aligned}\frac{d\,\sigma}{dY}(pp\to W^+X) \;=\; & K_W\frac{2\pi G_F}{3\sqrt{2}}x_1x_2\times\\ & \{|V_{ud}|^2\,[u(x_1)\bar{d}(x_2)+\bar{d}(x_1)u(x_2)]+|V_{us}|^2\,[u(x_1)\bar{s}(x_2)+\bar{s}(x_1)u(x_2)]\\ & +|V_{cs}|^2\,[c(x_1)\bar{s}(x_2)+\bar{s}(x_1)c(x_2)]+|V_{cd}|^2\,[c(x_1)\bar{d}(x_2)+\bar{d}(x_1)c(x_2)]\\ & +|V_{ub}|^2\,[u(x_1)\bar{b}(x_2)+\bar{b}(x_1)u(x_2)]+|V_{cb}|^2\,[c(x_1)\bar{b}(x_2)+\bar{b}(x_1)c(x_2)]\}\ ,\end{aligned}$$

$$\begin{aligned}\frac{d\,\sigma}{dY}(pp\to W^+X) \;=\; & K_W\frac{2\pi G_F}{3\sqrt{2}}x_1x_2\times\\ & \{|V_{ud}|^2\,[\bar{u}(x_1)d(x_2)+d(x_1)\bar{u}(x_2)]+|V_{us}|^2\,[\bar{u}(x_1)s(x_2)+s(x_1)\bar{u}(x_2)]\\ & |V_{cs}|^2\,[\bar{c}(x_1)s(x_2)+s(x_1)\bar{c}(x_2)]+|V_{cd}|^2\,[\bar{c}(x_1)d(x_2)+d(x_1)\bar{c}(x_2)]\\ & +|V_{ub}|^2\,[\bar{u}(x_1)b(x_2)+b(x_1)\bar{u}(x_2)]+|V_{cb}|^2\,[\bar{c}(x_1)b(x_2)+b(x_1)\bar{c}(x_2)]\}\ ,\end{aligned}\tag{2}$$

$$\begin{aligned}\frac{d\,\sigma}{dY}(pp\to ZX) \;=\; & K_Z\frac{2\pi G_F}{3\sqrt{2}}x_1x_2\times\\ & \{g_u^2[u(x_1)\bar{u}(x_2)+\bar{u}(x_1)u(x_2)+c(x_1)\bar{c}(x_2)++\bar{c}(x_1)c(x_2)]\\ & +g_d^2[d(x_1)\bar{d}(x_2)+\bar{d}(x_1)d(x_2)+s(x_1)\bar{s}(x_2)+\bar{s}(x_1)s(x_2)\\ & +b(x_1)\bar{b}(x_2)+\bar{b}(x_1)b(x_2)]\}\ ,\end{aligned}\tag{3}$$

where

$$\begin{aligned}g_u^2 \;&=\; (1-8\sin^2\theta_W/3+32\sin^4\theta_W/9)/2\ ,\\ g_d^2 \;&=\; (1-4\sin^2\theta_W/3+8\sin^4\theta_W/9)/2\ .\end{aligned}\tag{4}$$

Here G_F is the Fermi coupling constant, and $|V_{ij}|$ are the Cabibbo-Kobayashi-Maskawa (CKM) matrix elements. The factor $K_{W,Z}$ is the ratio of the next-to-leading order (NLO) to the leading order (LO) cross sections given by $K_{W,Z}\simeq 1+8\pi\alpha_s(M^2_{W,Z})/9$ [30]. The parton momentum fractions, x_1 and x_2 are related to rapidity Y by

$$x_1=\frac{M_{W,Z}}{\sqrt{s}}\ e^Y\ ,\quad x_2=\frac{M_{W,Z}}{\sqrt{s}}\ e^{-Y}\ ,\tag{5}$$

where $M_{W,Z}$ are the masses of the W and Z bosons. Thus, Y covers the range $-\ln(\sqrt{\mathrm{s}}/\mathrm{M_{W,Z}})$ to $\ln(\sqrt{\mathrm{s}}/\mathrm{M_{W,Z}})$. For numerical evaluation, we use $M_W=80.399$ GeV, $M_Z=91.188$ GeV, $G_F=1.166\times10^{-5}\,\mathrm{GeV}^{-2}$, and $\sin^2\theta_W=0.23$ [31].

For the evaluation of the rapidity distributions we use the NLO cross sections supplemented by the K-factor instead of evaluating the NNLO directly. As mentioned in the introduction, the PDFs and the partonic cross sections factorize in their dependence on the measured hadronic cross sections; our focus is on the constraints on the PDFs from the *ratio* of the differential cross sections. The charge asymmetry and the ratio of $d\sigma_{W^\pm}/d\sigma_Z$ are insensitive to the QCD corrections, therefore giving essentially the same results for different orders.

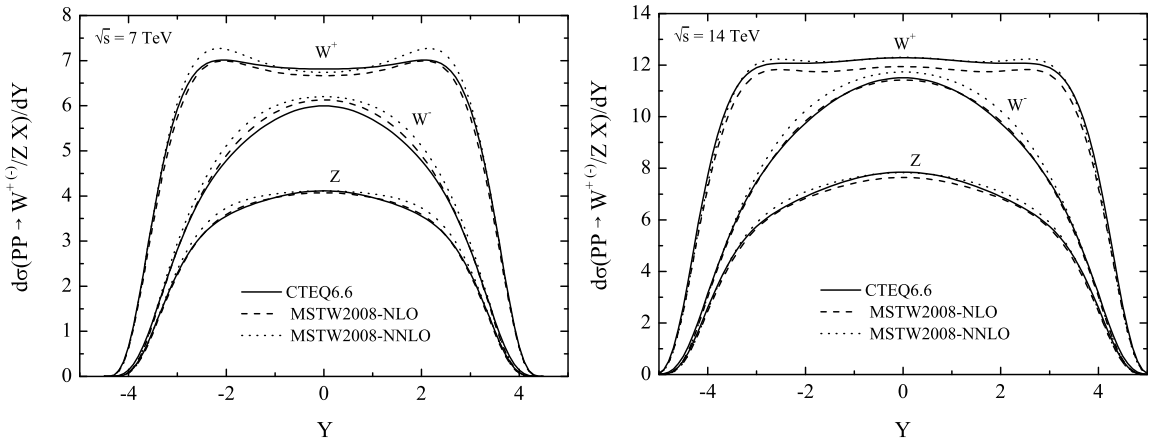

FIG. 2: The rapidity distribution of the differential cross sections for $W^\pm$ and Z boson production. The left and right figures are for energies of $\sqrt{s}$ = 7 TeV and $\sqrt{s}$ = 14 TeV, respectively. The results are presented for CTEQ6.6(solid) [32], MSTW2008-NLO(dashed) [29], and MSTW2008-NNLO(dotted) [29] PDFs.

The distribution of the differential cross sections in rapidity, evaluated following Eqs. 2–3, are shown in Fig. 2 for both the CTEQ6.6 [32] and MSTW2008 [29] PDFs, and for two different center-of-mass energy $\sqrt{s}$ = 7 and 14 TeV. The differential cross sections are symmetric with respect to the sign of the rapidity with $d\sigma_{W^\pm}(Y) = d\sigma_{W^\pm}(-Y)$, while $d\sigma_{W^-}(Y) = d\sigma_{W^+}(-Y)$ in $p\bar{p}$ collisions. The accessible rapidity range is $|Y| \lesssim 4.3$ at $\sqrt{s}$ = 7 TeV, and $|Y| \lesssim 5$ at $\sqrt{s}$ = 14 TeV allowing for the exploration of parton momentum fractions x as low as 1.7 $\times 10^{-4}$ and 4.2 $\times 10^{-5}$, respectively. The range of the rapidity and momentum fractions is much broader than for the Tevatron whose rapidity range from -3 to 3 probed minimum values of x_1 and x_2 of 2 $\times 10^{-3}$ at $\sqrt{s}$ = 1.96 TeV.

Fig. 3 shows the separate contributions from valence-sea and sea-sea interactions to the total differential cross sections for W, Z boson production. For the pp process, the

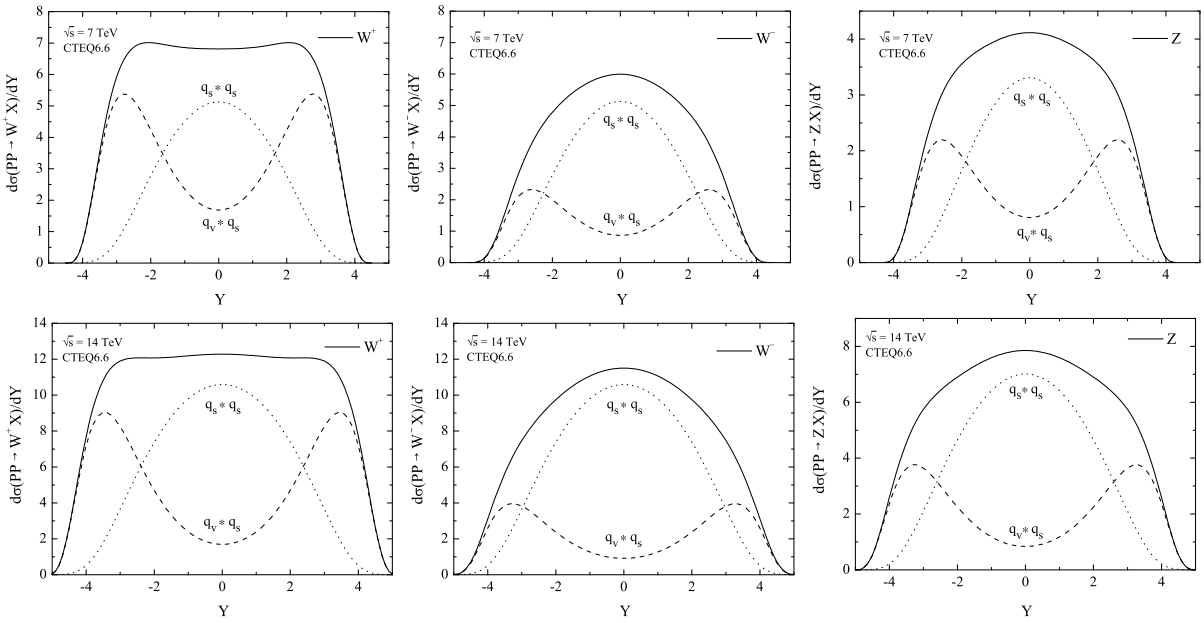

FIG. 3: The rapidity distribution of the differential cross sections for the production of weak bosons, $W^{\pm}$ and Z. The upper panels are for $\sqrt{s} = 7$ TeV and the lower panel for $\sqrt{s} = 14$ TeV. The contribution from valence-sea (dashed) and sea-sea (dotted) interactions are shown along with the total cross section (solid).

sea-sea interactions for W^+ and W^- are the same. As indicated in the figure, the sea-sea contributions are dominant in the central rapidity region, while the valence-sea contributions dominate in the forward and backward regions. The sea-sea contributions increase with collision energy. At rapidity zero the sea-sea process yields 75 % and 86 % of the W^+ and W^- production cross sections for $\sqrt{s} = 7$ TeV, and 86 % and 92 % for $\sqrt{s} = 14$ TeV. And we note that because the CKM elements squared have values of 0.95 for $|V_{ud}|^2$ and $|V_{cs}|^2$, and 0.05 for $|V_{us}|^2$ and $|V_{cd}|^2$, the valence-sea contributions are dominated by the $u_v\bar{d}$ channel for W^+ and $\bar{u}d_v$ for W^- production. For Z production, the sea-sea interactions yield 80 % and 89 % for $\sqrt{s} = 7$ and 14 TeV, respectively. Finally we note that the b quark interactions have an effect on the Z distributions as large as 4.1 % and 5.8 % in the central region, and contribute less than 1 % at $|Y| \gtrsim 2.5$ and $|Y| \gtrsim 3.3$ for $\sqrt{s} = 7$ TeV and 14 TeV, respectively. On the other hand, for W production, the b quark contributions are much more suppressed because of the small CKM matrix elements squared, with values of 10^{-5} for $|V_{ub}|^2$ and 2×10^{-3} for $|V_{cb}|^2$. Therefore, we can totally ignore the b quark contributions for the charge asymmetry of $W^{\pm}$ production, and safely ignore for the ratio of W/Z.

III. THE CHARGE ASYMMETRY OF $W^{\pm}$ PRODUCTION

In this section, we investigate the rapidity dependence of the charge asymmetry. The W^+ is produced mainly by the u and $\bar{d}$, and W^- by $\bar{u}$ and d channels. Since the PDFs of these quarks are different, a charge asymmetry appears in the W^+ and W^- production distributions, which is defined as

$$A_W(Y) \;=\; \frac{d\sigma_{W^+}/dY - d\sigma_{W^-}/dY}{d\sigma_{W^+}/dY + d\sigma_{W^-}/dY} \;. \tag{6}$$

The charge asymmetry in pp collision can be approximated in terms of the u and d quark distributions as

$$A(Y) \;\approx\; \left\{ \omega_1 \frac{u(x_1) - d(x_1)}{u(x_1) + d(x_1)} + \omega_2 \frac{u(x_2) - d(x_2)}{u(x_2) + d(x_2)} \right\} , \tag{7}$$

where the weight ω_1 and ω_2 are

$$\begin{aligned} \omega_1 \;&\equiv\; \frac{\frac{\bar{u}(x_2)+\bar{d}(x_2)}{u(x_2)+d(x_2)}}{\left[\frac{\bar{u}(x_1)+\bar{d}(x_1)}{u(x_1)+d(x_1)} + \frac{\bar{u}(x_2)+\bar{d}(x_2)}{u(x_2)+d(x_2)}\right]} \;, \\ \omega_2 \;&\equiv\; \frac{\frac{\bar{u}(x_1)+\bar{d}(x_1)}{u(x_1)+d(x_1)}}{\left[\frac{\bar{u}(x_1)+\bar{d}(x_1)}{u(x_1)+d(x_1)} + \frac{\bar{u}(x_2)+\bar{d}(x_2)}{u(x_2)+d(x_2)}\right]} \;. \end{aligned} \tag{8}$$

In Eq. 7 we made the approximation that $\bar{u}(x) = \bar{d}(x)$. As noted before, the b quark interactions contribute a negligible amount as a result of the very small values of the CKM matrix elements[1]. The weights ω_1 and ω_2 are shown in Fig. 4 as a function of W rapidity. Note that ω_1 and ω_2 both approach the value of 0.5 when $Y = 0$, i.e. $x_1 = x_2$. Also, ω_1 approaches 1 (0) for large positive (negative) rapidity, while ω_2 approaches 1 (0) for large negative (positive) rapidity.

The expression corresponding to Eq. 7 for $p\bar{p}$ collisions is given by [20]

$$A(Y) \;\sim\; D^{-1} \left[\frac{u(x_1) - d(x_1)}{u(x_1) + d(x_1)} - \frac{u(x_2) - d(x_2)}{u(x_2) + d(x_2)} \right] \;. \tag{9}$$

The multiplication factor has a value of 0.91 in the central region [20], in contrast with a value of 0.5 for the ω factors in pp collisions. From Eq. 9, it follows that $A(Y) = -A(-Y)$,

[1] We can perfectly neglect the c quark contribution to the numerator of $A(Y)$; however, in the denominator there are terms from $c\bar{s}$ and $\bar{c}s$ which cannot be ignored; they change the normalization. We use the original definitions, Eqs. (6) and (14), for our numerical presentation.

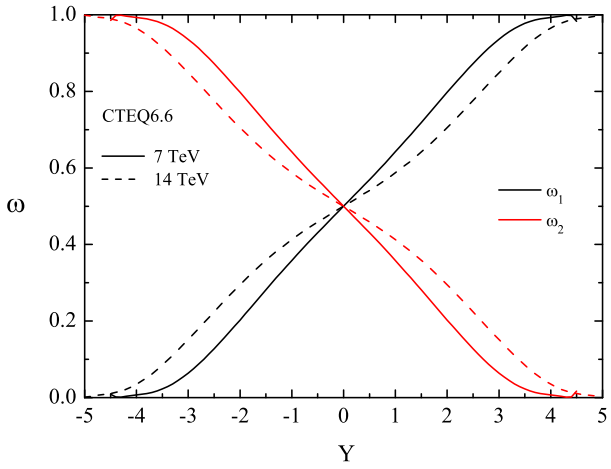

FIG. 4: The weights ω_1 (dark black) and ω_2 (bright red) as a function of rapidity for $\sqrt{s} = 7$ and 14 TeV.

while $A(Y) = A(-Y)$ for pp collisions. In summary, in $p\bar{p}$ collisions the W^+ distribution is symmetric with the W^- distribution, $d\sigma_{W^\pm}(Y) = d\sigma_{W^\mp}(-Y)$. Therefore, the rate of the two is the same at $Y = 0$. In contrast, in pp collisions, the rapidity distributions of W^+ and W^- are each symmetric with respect to rapidity, $d\sigma_{W^\pm}(Y) = d\sigma_{W^\pm}(-Y)$, and their magnitudes do not coincide at zero rapidity. Therefore, in the central region for pp collision

$$A(Y=0) \approx \frac{u(x)-d(x)}{u(x)+d(x)} \approx \frac{u_v(x)-d_v(x)}{u_v(x)+d_v(x)+2S(x)} , \tag{10}$$

with $S(x) = \bar{u}(x) = \bar{d}(x)$, where $x = M_W/\sqrt{s}$, while $A(Y = 0)$=0 in $p\bar{p}$ collisions. This difference makes the determination of u/d possible using pp data.

Inclusively produced weak bosons decay to leptons, $W \to l\nu_l$ and $Z \to l\bar{l}$, and the rapidity $Y_{W,Z}$ are reconstructed from the energy (E_l) and the longitudinal momentum ($p_{l,L}$) of the secondary leptons. The rapidity of the Z boson can be fully reconstructed from the measurement of its decay products. In contrast, the W rapidity cannot be reconstructed because the longitudinal momentum of the neutrino is not measured. We therefore reconstruct the W rapidity from the momentum of the charged lepton and the (indirectly determined) transverse momentum of neutrino [26]. We introduce the definitions

$$Y_\pm = \frac{1}{2}\ln\frac{E_l + p_{l,L} + p_{\nu_l,T}e^{Y_{\nu_\pm}}}{E_l - p_{l,L} + p_{\nu_l,T}e^{-Y_{\nu_\pm}}}, \tag{11}$$

where

$$Y_{\nu_\pm} = Y_l \pm \ln[1 + \delta + \sqrt{\delta(2+\delta)}], \tag{12}$$

with

$$\delta = \frac{M_W^2 - M_T^2}{2p_{l,T}p_{\nu_l,T}} \ . \tag{13}$$

Here M_T^2 is the transverse mass of the lepton and neutrino defined as $M_T^2 = (|p_{l,T}|+|p_{\nu,T}|)^2 - (p_{l,T} + p_{\nu,T})^2$.

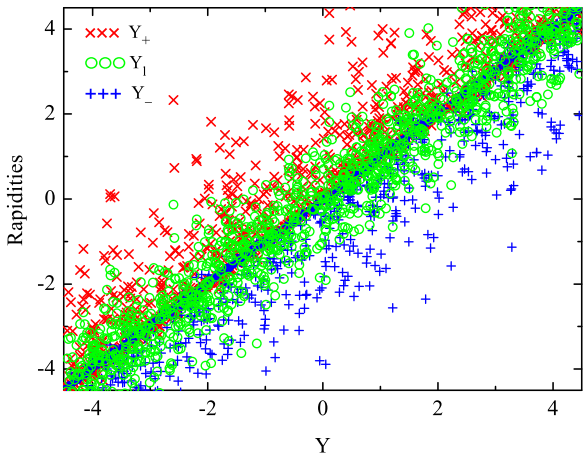

FIG. 5: The distributions of the reconstructed rapidities $Y_\pm$ and the charged lepton rapidity Y_l as function of Y.

Fig. 5 shows the distribution of the reconstructed rapidity $Y_\pm$ and the charged lepton rapidity Y_l as a function of the rapidity of W. Y_l and $Y_\pm$ are related: $Y_l = (Y_+ + Y_-)/2$. In the massless limit, the lepton rapidity Y_l is the same as the pseudorapidity η, which is used to investigate the lepton charge asymmetry [23, 25, 34–42]. As indicated in Fig. 5, Y_l correlates roughly with the rapidity Y, therefore, Y_l could also be an approximate optional choice for Y. In this paper, however, we use the experimentally fully reconstructible $Y_\pm$ to investigate the charge asymmetry and the ratio of W/Z.

The *experimentally reconstructed rapidity* $Y_\pm$ has a twofold ambiguity because of the two solutions for $Y_{\nu_\pm}$ from Eq. 12. This can be displayed by comparing the $Y_\pm$ and Y distributions: Fig. 6 shows the differential cross sections for W^+ and W^- as a function of Y and Y_- at $\sqrt{s} = 7$ TeV and 14 TeV. Thus, we can chose either Y_+ or Y_- as the appropriate observable to study the charge asymmetry. In this paper, we take Y_- and will therefore present results for the positive rapidity range only. In Fig. 6 the solid lines show the Y distributions, while the dashed and dotted lines show the Y_- distributions with the transverse momentum limited.

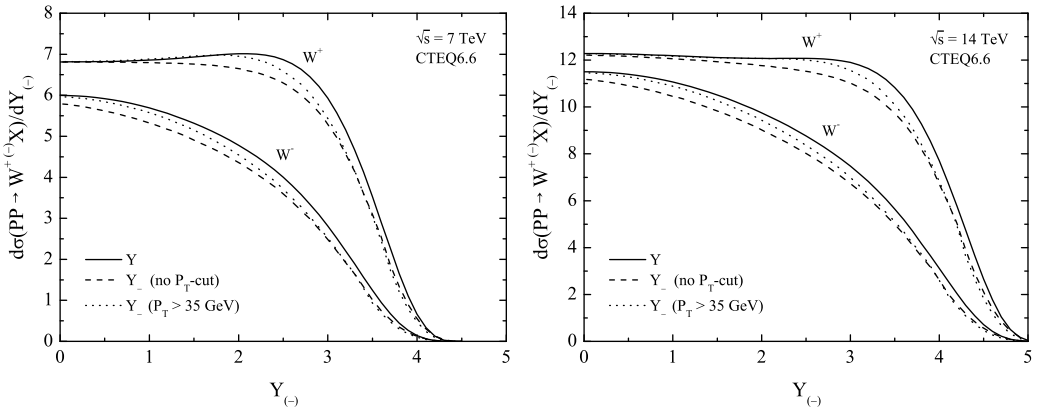

FIG. 6: The differential cross section for W^+ and W^- as function of the rapidity. The solid lines indicate the distributions for the real rapidity of the W boson, while the dashed lines are for the reconstructed rapidity Y_- with or without the P_T cut.

We can now redefine the W charge asymmetry $A(Y)$ in terms of the reconstructed rapidity $Y_\pm$ as

$$A(Y) \;=\; \frac{d\sigma_{W^+}/dY_{-(+)} - d\sigma_{W^-}/dY_{-(+)}}{d\sigma_{W^+}dY_{-(+)} + d\sigma_{W^-}/dY_{-(+)}}\;, \tag{14}$$

for $Y > 0$ ($Y < 0$). The results for the asymmetry following Eq. 14 are presented in Fig. 7 for different sets of PDFs. For this numerical evaluation, we have included all flavors in Eq. 2. We note that the results for the NLO PDFs (red solid) [29] and NNLO PDFs (blue

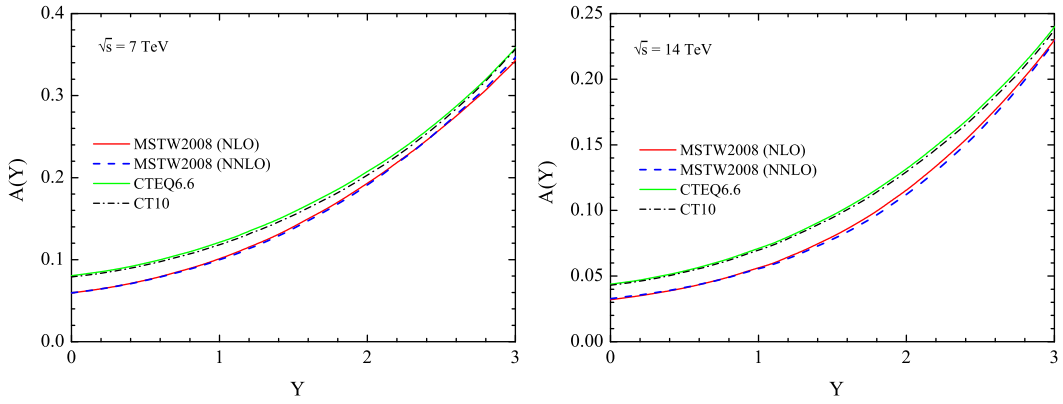

FIG. 7: The charge asymmetry $A(Y)$ for the different PDFs for energies of $\sqrt{s} = 7$ and 14 TeV as a function of the reconstructed rapidity Y_-. The results for the PDFs are differentiated by color: red for MSTW2008-NLO [29], blue for MSTW2008-NNLO [29], green for CTEQ6.6 [32] and black for CT10 [33].

dashed) [29] are essentially degenerate, as expected.

IV. CHARM QUARK DISTRIBUTIONS OF THE PROTON

As shown in sec. II, sea-sea quark contributions significantly contribute to LHC rapidity distributions of the weak bosons. We will focus next on the charm contributions $c\bar{s}$ and $c\bar{d}$ ($\bar{c}s$ and $\bar{c}d$) for $W^+(W^-)$ and of $c\bar{c}$ for Z.

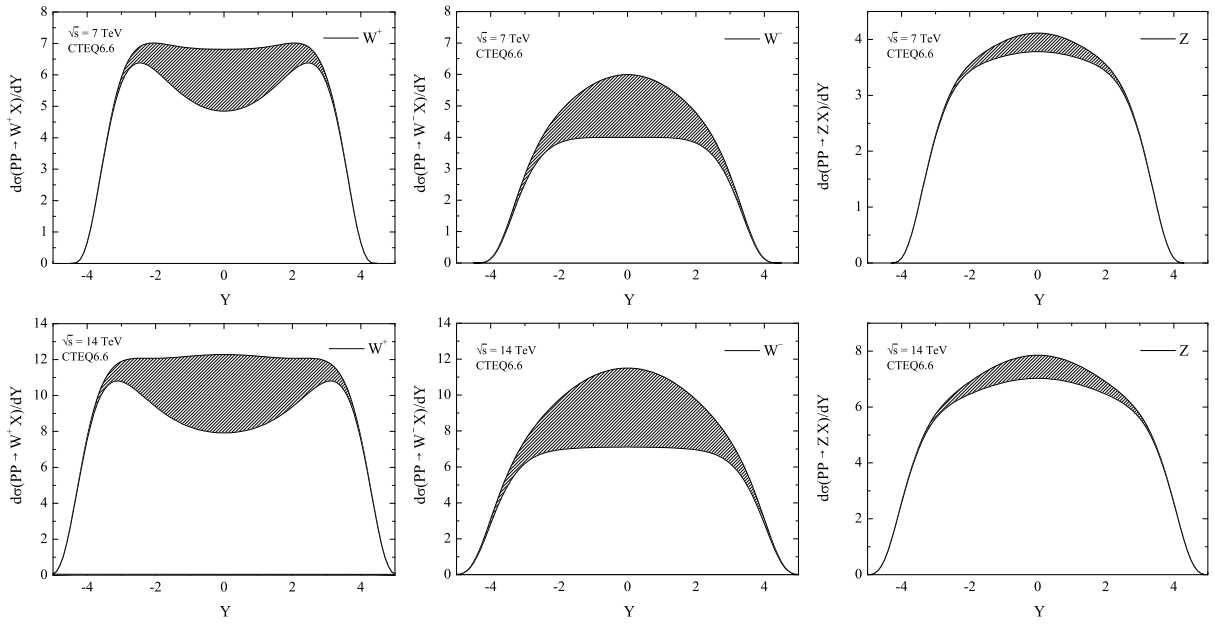

FIG. 8: The charm quark contribution to the rapidity distribution of $d\sigma/dY$ for the production of W^+, W^-, and Z boson with $\sqrt{s} = 7$ TeV and 14 TeV.

The shaded area in Fig. 8 displays the charm quark contributions to the weak boson rapidity distributions. As already mentioned, for W production the terms proportional to $|V_{cd}|^2$ are quite small and therefore the dominant subprocess is $c\bar{s}$ ($s\bar{c}$) for W^+ (W^-). This charm contribution dominates in the central region and contributes 29% to W^+, 33% to W^-, and 8% to Z production cross sections at $\sqrt{s} = 7$ TeV. At 14 TeV its influence increases to 36%, 38%, and 11%, respectively.

In this section, we will investigate the charm PDF using the ratio of the W and Z differential rapidity distributions. We redefine the quantity $B(Y)$, introduced in Ref. [26] for $p\bar{p}$ collisions, in terms of the experimentally reconstructed rapidity as

$$B(Y) = \frac{d\sigma_{W^+}/dY_- + d\sigma_{W^-}/dY_-}{d\sigma_Z/dY} \ . \tag{15}$$

$B(Y)$ is shown in Fig. 9 for different PDFs. As is the case for the charge asymmetry, the values of $B(Y)$ evaluated with MSTW2008-NLO PDFs [29] and MSTW2008-NNLO [29] are almost identical. The effect of the cut $P_T > 35$ is shown by the dashed lines. The values of B(Y) are 3.05 - 3.11 for the CTEQ6.6 PDFs [32], and 3.07- 3.10 for MSTW2008 for $|Y| < 2$ at $\sqrt{s} = 7$ TeV. At $\sqrt{s} = 14$ TeV, they are slightly reduced, to 2.96 - 3.11 for CTEQ PDFs, and 2.99 - 3.09 for MSTW PDFs in the range $|Y| < 3$. The results with the transverse momentum P_T applied differ by 1.3% - 4.3% for $|Y| < 2$ at $\sqrt{s} = 7$ TeV, and 1.3% - 4.4% for $|Y| < 3$ at $\sqrt{s} = 14$ TeV.

In Fig. 10, $B(Y)$, given by Eq. 15, is shown as a function of the charm contribution ϵ, which is defined as

$$\epsilon \equiv \frac{c(x)}{((\bar{u}(x) + \bar{d}(x))/2)} = \frac{2c(x)}{(\bar{u}(x) + \bar{d}(x))} \ . \tag{16}$$

No cut on the transverse momentum p_T is applied. Because the NNLO set gives almost the same results as the NLO for MSTW PDFs [29], we only show the results for the NLO PDFs. Comparing the results with and without the contributions of charm we find that ϵ has a value of 0.5 -0.75.

In addition to $B(Y)$, we calculate the the ratio of the integrated cross sections, $B(\epsilon)$,

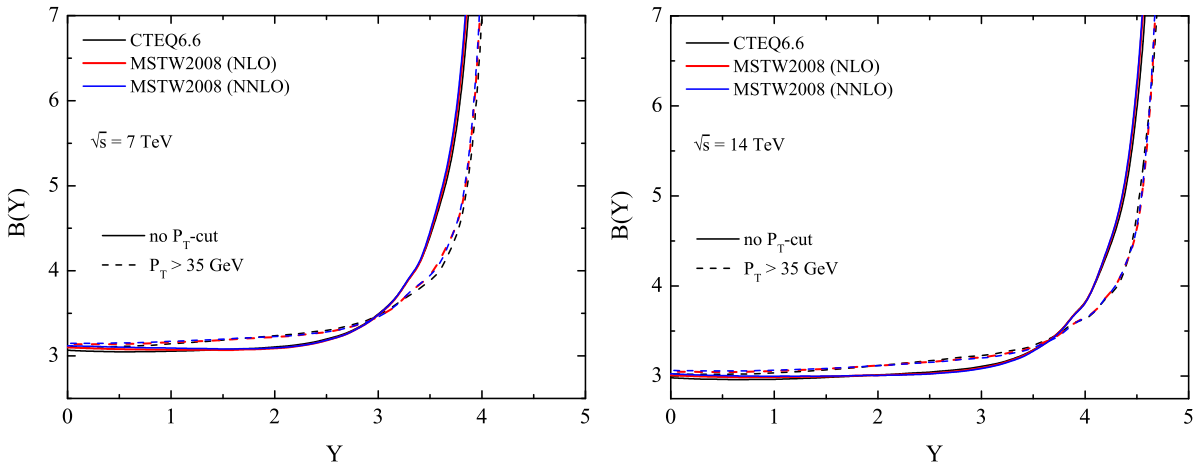

FIG. 9: $B(Y)$ as a function of rapidity for $\sqrt{s} = 7$ and 14 TeV. The distributions without P_T cut are displayed by solid lines while the results evaluated with $P_T > 35$ GeV are shown as dashed lines. As in Fig. 7, the CTEQ6.6 PDF [32] results are shown in black, MSTW2008-NLO [29] red, and MSTW2008-NNLO [29] as blue solid lines.

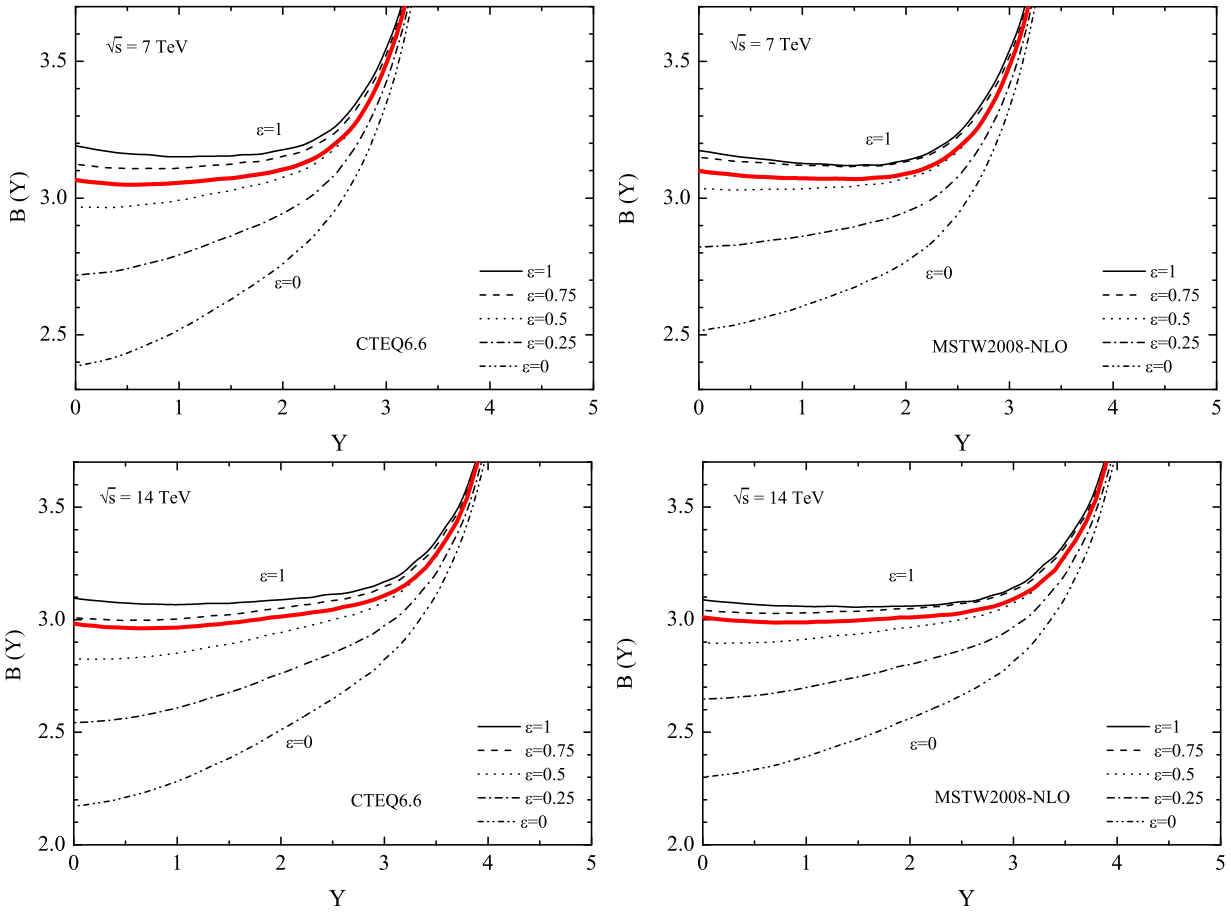

FIG. 10: $B(Y)$ as a function of ϵ ($\epsilon = 2c(x)/(\bar{u}(x) + \bar{d}(x))$) for $\sqrt{s} = 7$ and 14 TeV. The CTEQ6.6 and MSTW 2008-NLO PDF sets are used. The red solid lines show the results including the charm structure function in the sample PDFs.

which is given by

$$B(\epsilon) = \int_{\text{with } Y \text{ cut}} \frac{d\sigma_{W^+}/dY_- + d\sigma_{W^-}/dY_-}{d\sigma_Z/dY} \ . \tag{17}$$

The result is displayed in Fig. 11 as function of ϵ. $B(\epsilon)$ is evaluated for $|Y| = 1$ and 3 for $\sqrt{s} = 7$ TeV, and 2 and 4 for 14 TeV. The crosses in the figure indicate the $B(\epsilon)$ values evaluated with the charm distributions from the PDF sets. For example, $B(\epsilon)$ evaluated for $|Y| < 3$ is 3.07 for CTEQ6.6 [32] and 3.08 for MSTW2008 PDFs [29] at $\sqrt{s} = 7$ TeV. At $\sqrt{s} = 14$ TeV, we find 3.06 for both PDFs for $|Y| < 4$. These values yield ϵ 0.63 to 0.60 at $\sqrt{s} = 7$ TeV, and 0.68 to 0.66 at 14 TeV for the CTEQ6.6 and MSTW2008 PDF sets, respectively.

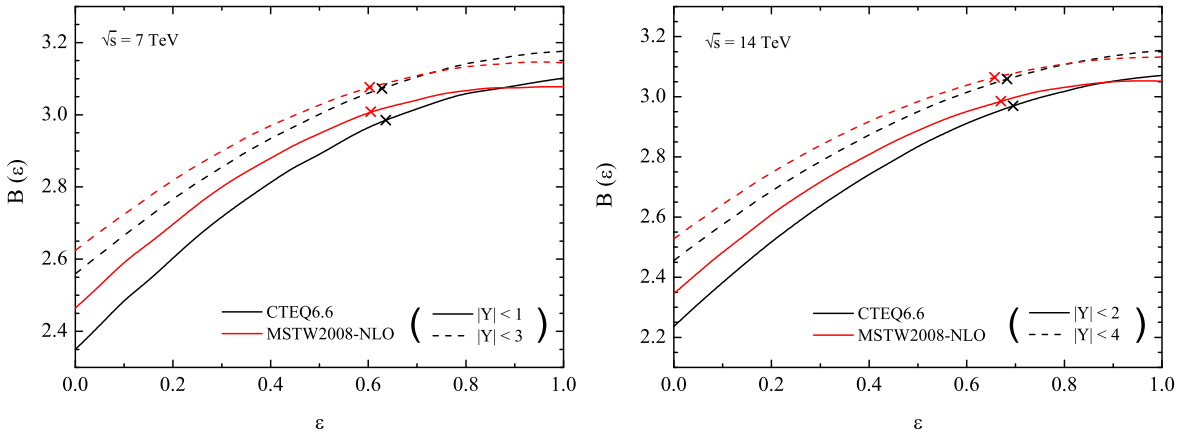

FIG. 11: The ratio of the integrated cross sections $B(\epsilon)$ as a function of ϵ for different ranges of Y. The values of $B(\epsilon)$ evaluated with the charm distributions from each sample PDF are represented by the crosses.

V. SUMMARY AND CONCLUSIONS

Using sample PDFs, we have examined the charge asymmetry for u and d quarks as well as the ratio of cross sections $B(Y)$ and $B(\epsilon)$ in the experimentally accessible weak boson rapidity range at the LHC. We subsequently focused on the role of charm quark contributions. For the charge asymmetry the effects of the heavy quark PDFs $c(x)$ and $b(x)$ are negligible, even at the highest energy. One can therefore isolate and explore the $u(x)$ and $d(x)$ (or $u_v(x)$ and $d_v(x)$) structure functions. In this context, we presented a simplified expression of the charge asymmetry in terms of the u and d distribution functions.

We also studied the charm contribution $\epsilon = 2c(x)/(\bar{u}(x) + \bar{d}(x))$ to $B(Y)$ and $B(\epsilon)$. The CTEQ6.6 [32] and MSTW2008 PDF [29] sets indicate a value of ϵ of about 0.6 for $\sqrt{s} =$ 7 TeV, and $\sim$ 0.7 for 14 TeV. The measurement of the rapidity distributions of W/Z (or $B(Y)$) interpreted in terms of $B(Y)$ and $B(\epsilon)$ will lead to a straightforward determination of the charm quark component of the the sea quarks at the LHC.

Acknowledgments

The work was supported by the National Research Foundation of Korea (NRF) grant funded by Korea government of the Ministry of Education, Science and Technology (MEST) (No. 2011-0017430) and (No. 2011-0020333). The work of F. H. is supported in part by the

National Science Foundation under Grants No. OPP-0236449 and and PHY-0969061, and in part by the University of Wisconsin Alumni Research Foundation.

[1] S. D. Drell and T. M. Yan Phys. Rev. Lett. **25**, 316 (1970); **25**, 902 (1970) .

[2] F. Abe *et al.*, CDF Collaboration Phys. Rev. Lett. **69**, 28-32 (1992)

[3] F. Abe *et al.*, CDF Collaboration Phys. Rev. Lett. **73**, 220-224 (1994)

[4] F. Abe *et al.*, CDF Collaboration Phys. Rev. Lett. **76**, 3070 (1996)

[5] B. Abbott *et al.*, D0 Collaboration Phys. Rev. D. **60**, 052003 (1999).

[6] B. Abbott *et al.*, D0 Collaboration Phys. Rev. D. **61**, 072001 (2000).

[7] T. Affolder *et al.*, CDF Collaboration Phys. Rev. Lett. **85**, 3347 (2000)

[8] T. Affolder *et al.*, CDF Collaboration Phys. Rev. D. **64**, 052001 (2001)

[9] V. M. Abazov *et al.*, D0 Collaboration Phys. Rev. D. **66**, 032008 (2002)

[10] V. M. Abazov *et al.*, D0 Collaboration Phys. Rev. D. **66**, 012001 (2002)

[11] D. Acosta *et al.*, CDF Collaboration Phys. Rev. Lett. **94**, 091803 (2005).

[12] D. Abulencia *et al.*, CDF Collaboration J. Phys. G. **34**, 2457-2544 (2007).

[13] V. M. Abazov *et al.*, D0 Collaboration Phys. Rev. Lett. **101**, 191801 (2008).

[14] B. Abbott *et al.*, D0 Collaboration Phys. Rev. Lett. **103**, 231802 (2009).

[15] G. Aad, The ATLAS Collaboration, JHEP **12**, 060 (2010);

[16] V. Khachatryan, The CMS Collaboration, JHEP **01**, 080 (2011); S. Chatrchyan, JHEP **10**, 132 (2011).

[17] G. Aad, The ATLAS Collaboration, Phys. Rev. D. **85**, 072004 (2012).

[18] R. Hamberg, W. L. van Neerven, abd T. Matsuura, Nucl. Phys. **B359**, 343 (1991); **B644**, 403 (2002) .

[19] C. Anastasiou, L. Dixon, K. Melnikov, and F. Petriello, Phys. Rev. D. **69**, 094008 (2004).

[20] E. L. Berger, F. Halzen, C. S. Kim and S. Willenbrock, Phys. Rev. D **40**, 83 (1989).

[21] A. Bodek, Y. Chung, B. Y. Han, K. McFarland, and E. Halkiadakis, Phys. Rev. D **77**, 111301 (2008).

[22] T. Aaltonen, The CDF Collaboration, Phys. Rev. Lett. **102**, 181801 (2009).

[23] S. Catani, G. Ferrera and M. Grazzini, JHEP **05**, 006 (2010).

[24] K. Lohwasser, J. Ferrando and C. lssever, JHEP **09**, 079 (2010).

[25] L. T. Brady, A. Accardi, W. Melnitchouk and J. F. Owens, JHEP **06**, 019 (2012).

[26] K. Hagiwara, F. Halzen, and C. S. Kim, Phys. Rev. D **41**, 1471 (1990).

[27] A. Kusina *et al.*, Phys. Rev. D. **85**, 094028 (2012).

[28] The ATLAS Collaboration, Phys. Rev. Lett. **109**, 012001 (2012).

[29] A. D. Martin, W. J. Stirling, R. S. Thorne, and G. Watt, Eur. Phys. J. **C63**, 189 (2009).

[30] V. Barger and R. J. N. Phillips, *Collider Physics*, Addison-Wesley (1987).

[31] K. Nakamura *et al.* (Particle Data Group), J. Phys. G. **37**, 075021 (2010).

[32] P. M. Nadolsky *et al.*, Phys. Rev. D. **78** 013004 (2008).

[33] H. -L. Lai *et al.*, Phys. Rev. D. **82** 074024 (2010).

[34] W. Melnitchouk and J. Peng, Phys. Lett. B. **400** 220 (1997).

[35] F. Abe, The CDF Collaboration, Phys. Rev. Lett. **81**, 5754-5759 (1998).

[36] A. Bodek *et al.*, Phys. Rev. Lett. **83**, 2892-2895 (1999).

[37] D. Acosta, The CDF Collaboration, Phys. Rev. D **71**, 051104 (2005).

[38] V. M. Abazov, The D0 Collaboration, Phys. Rev. D **77**, 011106 (2008).

[39] V. M. Abazov, The D0 Collaboration, Phys. Rev. Lett **101**, 211801 (2008).

[40] G. Aad, The ATLAS Collaboration, Phys. Lett. B **701**, 31-49 (2011).

[41] S. Chatrchyan, The CMS Collaboration, JHEP **04**, 050 (2011).

[42] S. Chatrchyan, The CMS Collaboration, Phys. Rev. Lett. **109**, 111806 (2012).